BeBeC-2018-S10

ACOUSTIC BEAMFORMING BY NON-SYNCHRONOUS MICROPHONE ARRAY MEASUREMENTS

Liang Yu[1], Weikang Jiang[1], Jerome Antoni[2], Quentin Leclere[2] and Haijun Wu[1]
[1]State Key Laboratory of Mechanical System and Vibration
Shanghai Jiao Tong University, Shanghai 200240, China
[2]Laboratory Vibrations and Acoustics, INSA-Lyon
Batiment St. Exupery 25 bis av. Jean Capelle, 69621 Villeurbanne cedex - France

Abstract

Acoustic beamforming consists in measuring the sound field by the microphone array and infers the source strength in conjunction with the propagation model. A fundamental limitation of acoustic beamforming is determined by the aperture size of the array and the microphone density. In order to extend the working frequency range of conventional phased array beamforming, the sound sources are scanned by moving sequentially a small prototype array, resulting in a large array and high microphone density measurements, which is referred to as non-synchronous measurements beamforming. The main issue of non-synchronous measurements beamforming is that the phase relationships between consecutive snapshots of non-synchronous measurements are missing and result in missing entries in the spectral matrix, however, complete spectral matrix information is crucial for high quality image of beamforming. Thus, non-synchronous measurements beamforming boils down to a spectral matrix completion problem which is modeled by a structured low rank model and solved by designed fast iteration algorithm. In particular, the structured low rank model is constructed by two ingredients: (1) the low rank property of the spectral matrix and (2) the continuity of the acoustic field. The simulation results show the non-synchronous measurements beamforming extended the working frequency range of given small phased array from $2-2.8$ kHz to $1.6-4.5$ kHz with only 9 times non-synchronous measurements.

1 INTRODUCTION

Acoustic imaging aims to obtain a visualized sound map from the radiating objects, which has a wide range of applications in source identification, vibration analysis and machine diagnosis

[9, 13]. It is generally accepted that the beamforming [4, 10] and Near-field Acoustical Holography (NAH) [15] are two most widely exploited methods dedicated to the aforementioned issues. A fundamental limitation of acoustic source imaging is imposed by geometry of the array. Specifically, the minimum frequency of reconstruction depends on the dimension of the array and the maximum frequency depends on the distance between neighboring microphones [5]. A solution to achieve a large array and/or high microphone density is to scan the object of interest by moving sequentially a prototype array (an arbitrary array of achieving the sequential measurements), which is referred to as non-synchronous measurements. Non-synchronous measurements have been addressed in [2, 8, 11] in the context of NAH, which breaks through the restriction of using references by reconstructing the phase from the quadratic pressure and tangential components of the sound intensity, yet it requires the use of an array of intensity probe.

The non-synchronous measurements in the context of NAH was further investigated in Ref [1] by taking the incomplete measurements explicitly into account to formulate the acoustic inverse problem, which is recognised an intrusive method since it directly solves the inverse problem with the incomplete measurements and requires manipulation of the structure of current reconstruction methods. Non-intrusive method of non-synchronous measurements has been next investigated in Ref [7], which is reformulated as a matrix completion problem, and the Cyclic Projection (CP) [16] and FISTA [17] algorithm were proposed correspondingly to find a full spectral matrix subject to given constraint of hermitian symmetry, measurement fitting, reduced rank and spatial continuity of the sound field. The non-intrusive method aims to complete a spectral matrix, then feeds it to the spectral matrix based acoustic image method.

However, there remains a need for an efficient beamforming method of non-synchronous measurements. The spectral matrix completion in the context of beamforming is still dissimilar with the one in NAH. First, The beamforming demands a fast and robust implementation of spectral matrix completion, whereas the NAH requests a high accuracy implementation of spectral matrix completion. The different challenges of computational efficiency and accuracy will result in various choices of nuclear norm minimization algorithms. Second, the beamforming is usually implemented in the far field and the NAH in the near field, and the measurements distances are highly connected with the spatial basis choices in spectral matrix completion. Thus, the differences between the NAH and beamforming result in the different methods of spectral matrix completion of data missing from the aspects of interpolation basis choices and the nuclear norm minimization algorithms.

In this paper, the non-synchronous measurements in the context of beamforming is formally formulated as the problem of spectral matrix completion, which is solved by the Fast Iterative Shrinkage Thresholding Algorithm. The paper is organized as follows. The Forward model of sound propagation and acoustic beamforming is described in section 2, and the spectral matrix completion with nuclear norm minimization is given in section 3. Section 4 and 5 are separately the simulation and conclusion.

2 FORWARD MODEL OF SOUND PROPAGATION AND ACOUSTIC BEAMFORMING

2.1 Conventional beamforming

Assume the source plane is equally discretized into N grids at the known positions $\mathbf{r}_n$, $n = 1,...,N$, and S incoherent broadband sound sources with coordinates $\mathbf{r}_s$, $s = 1,...,S$ are distributed on these grids (the position set $\{\mathbf{r}_s\}$ belongs to the set $\{\mathbf{r}_n\}$). The radiated sound is measured by M microphones ($N > M > S$) with coordinates $\mathbf{r}_m$, $m = 1,...,M$. The measured sound pressures in the time domain are modeled as stochastic processes, then a number of snapshots are produced by the Fourier transform of a short-time segment tapered with a smooth data window. The M dimensional vector of measured pressures $\mathbf{p}_t = (p_{1t},...,p_{Mt})^T$ at a frequency f corresponding to the t-th snapshot ($t = 1,...,T$) is obtained by:

$$\mathbf{p}_t = \mathbf{G}(r)\mathbf{s}_t^* + \mathbf{n}_t. \tag{1}$$

Here, the $M \times S$ matrix $\mathbf{G} = (\mathbf{g}_1,...,\mathbf{g}_s,...,\mathbf{g}_S)$, in which a general term g_{ms} describes the free-field sound propagation model from the s-th source to the m-th microphone:

$$g_{ms} = G(r_m|r_s) = \frac{e^{jk\|r_m - r_s\|}}{4\pi\|r_m - r_s\|}, \tag{2}$$

where $k = \frac{2\pi f}{c}$ is the wavenumber and c is the sound speed. The vector $\mathbf{s}_t^* = (s_{1t}^*,...,s_{St}^*)^T$ contains the uncorrelated random amplitudes of the sound sources: it is assumed to follow an S dimensional complex-valued Gaussian distribution with $\mathbf{0}$-mean and diagonal covariance matrix

$$\mathbf{S}_{cc}^* = \mathbb{E}\{\mathbf{s}_t^*\mathbf{s}_t^{*H}\} = \mathrm{diag}(\boldsymbol{\alpha}^2), \tag{3}$$

where $\boldsymbol{\alpha}^2 = (\alpha_1^2,...,\alpha_S^2)^T$ is vector of powers (variances of amplitudes) of the sound sources and $\mathrm{diag}(\mathbf{x})$ denotes the diagonal matrix with the elements of $\mathbf{x}$ on the main diagonal. The measurement noise vector $\mathbf{n}_t = (n_{1t},...,n_{Mt})^T$ is also assumed to be complex Gaussian distributed with $\mathbf{0}$-mean and covariance matrix $\mathbf{S}_{nn} = \sigma^2\mathbf{I}_M$. It is reasonable to further assume that s_{t_1} and n_{t_2} are independent for any two snapshots $t_1, t_2 \in \{1,...,T\}$. Therefore, the sound pressure $\mathbf{p}_t$ measured by a microphone array follows a complex-valued multivariate Gaussian distribution with $\mathbf{0}$-mean and spectral matrix of propagation is

$$\mathbf{S}_{pp} = \mathbb{E}\{\mathbf{p}_t\mathbf{p}_t^H\} = \mathbf{G}\mathbf{S}_{cc}^*\mathbf{G}^H + \mathbf{S}_{nn} = \mathbf{G}\mathrm{diag}(\boldsymbol{\alpha}^2)\mathbf{G}^H + \sigma^2\mathbf{I}_M. \tag{4}$$

Conventional beamforming consists in estimating the S sources by the sound pressures measured by the M microphones, and the parameters to estimate are the locations $\mathbf{r}_s$ and the powers $\boldsymbol{\alpha}_s^2$ ($s = 1,...,S$) of the sound sources. The conventional beamforming is based on the assumption that the signals are emitted by a single source of the discretized source plane $\mathbf{r}_n$. Thus the forward model of Eq. (1) can be further written as a discrete forward model of signal propagation:

$$\mathbf{p}_t = \mathbf{G}(r)\mathbf{s}_t + \mathbf{n}_t. \tag{5}$$

Here $\mathbf{G}(r)$ is $M \times N$ matrix with $\mathbf{G} = (\mathbf{g}_1, ..., \mathbf{g}_n, ..., \mathbf{g}_N)$, in which a general term g_{mn} describes the free-field sound propagation model from the n-th source to the m-th microphone:

$$g_{mn} = G(r_m|r_n) = \frac{e^{jk\|r_m - r_n\|}}{4\pi\|r_m - r_n\|}. \tag{6}$$

The idea behind each beamformer is to steer the microphone array to search for the source position, and the beamformer power output $B(\mathbf{r}_n = \mathbf{r}_s)$ at position $\mathbf{r}_n$ of measurement $\mathbf{p}_t$ is defined as

$$\begin{cases} B(\mathbf{r}_n = \mathbf{r}_s) = \mathbf{w}_n^H \hat{\mathbf{S}}_{pp} \mathbf{w}_n, \text{ where } \hat{\mathbf{S}}_{pp} = \frac{1}{T}\sum_{t=1}^{T} \mathbf{p}_t \mathbf{p}_t^H \\ \mathbf{w}_n = \frac{\mathbf{g}_n}{\|\mathbf{g}_n\|_2^2}, n = 1, ..., N \end{cases} \tag{7}$$

The weights $\mathbf{w}_n = \frac{\mathbf{g}_n}{\|\mathbf{g}_n\|_2^2}$ are designed to be independent of the array data or data statistics, which compensate the time delays and amplitude attenuation of the forward propagation.

2.2 Forward model of non-synchronous microphone array measurements

The non-synchronous microphone array measurements are achieved by scanning the sound sources (moving sequentially the prototype array), then the sound image is obtained by the conventional beamforming. Thus, the i-th measurement of non-synchronous microphone array measurements is modeled as the same propagation of Eq. (1),

$$\mathbf{p}_t^{\{i\}} = \mathbf{G}^{\{i\}}(r)\mathbf{s}_t^* + \mathbf{n}_t. \tag{8}$$

where $i = 1, ..., P$ and P is the number of non-synchronous array measurements. The spectral matrix model of propagation in Eq. (4) can then be correspondingly reformulated as the non-synchronous measurements form

$$\mathbf{S}_{pp}^{(i)} = \mathbb{E}\{\mathbf{p}_t^{\{i\}} \mathbf{p}_t^{\{i\}^H}\} = \mathbf{G}^{\{i\}} \mathbf{S}_{cc}^* \mathbf{G}^{\{i\}^H} + {\beta_i}^2 \mathbf{I}_M, \quad i = 1, ..., P, \tag{9}$$

where the noise power ${\beta_i}^2, i = 1, ..., P$ is estimated for each configuration i but equal for all sensors. The estimated spectral matrix is calculated by $\hat{\mathbf{S}}_{pp}^{(i)} = \frac{1}{T}\sum_{t=1}^{T} \mathbf{p}_t^{\{i\}} \mathbf{p}_t^{\{i\}^H}$. It is noted that the $\mathbf{S}_{cc}^*$ is invariant for measurements mode since the fundamental premise of the acoustic source distribution is considered as a stationary stochastic field in this paper. The spectral matrices $\hat{\mathbf{S}}_{pp}^{(i)}$, $i = 1, ..., P$ of each with size $M \times M$ can be methodically rearranged in the block diagonal positions of an incomplete spectral matrix $\hat{\mathbf{S}}_{pp}^{m}$ of $MP \times MP$ (see left part of Fig. 1). Contrary to non-synchronous measurements, spectral matrix $\hat{\mathbf{S}}_{pp}$ of simultaneous measurement (assumes the number of microphone in Eq. (1)) is MP) is a full matrix with size $MP \times MP$ since all the coherence information of array measurements are known. With the purpose of using non-synchronous measurements for acoustic beaforming, the problem is formulated as to seek an full spectral matrix from the spectral matrix $\hat{\mathbf{S}}_{pp}^{m}$ of data missing.

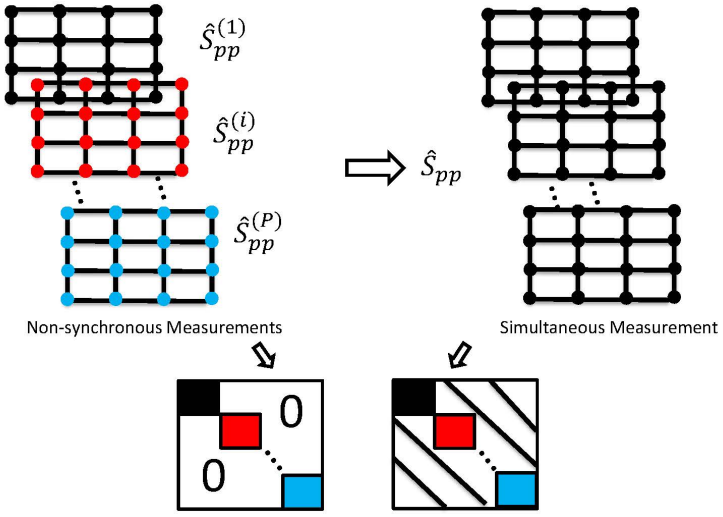

Figure 1: measurement mode and spectral matrix: non-synchronous measurements (left) versus simultaneous measurement (right).

3 SPECTRAL MATRIX COMPLETION WITH NUCLEAR NORM MINIMIZATION

3.1 Low rank modeling of acoustic field

In acoustics, the rank of spectral matrix measures the stochastic complexity of the acoustic field that is produced by the uncorrelated sources (latent variables in stochastic terminology), and it indicates the number of uncorrelated sources. That is to say, although the measured sound field (usually with measurements noise) might look complicated, it is assumed that the observed sound field is only radiated from limited number of sound sources, and many piratical acoustic scenarios have justified this assumption. This limited number of uncorrelated sources produce a correlated sound field, and the rank of spectral matrix can be used to measure the correlation of the acoustical field. For instance, a rank one spectral matrix corresponds to a fully coherent field (the measurement in one position can be easily predicted from other positions in the field), whereas a spectral matrix with full rank corresponds to a diffuse field in general. Thus, the spectral matrix completion problem boils down to seeking a spectral matrix with low rank (minimized rank) subject to a given constraint of hermitian symmetry and corresponding

measurements of missing, i.e.

$$\begin{aligned} \underset{\mathbf{S}}{\text{minimize}} \quad & \text{Rank}(\mathbf{S}) \\ \text{subject to} \quad & \|\mathscr{A}(\mathbf{S}) - \hat{\mathbf{S}}_{pp}^{m}\|_F \leq \varepsilon \\ & \mathbf{S}^* = \mathbf{S} \succeq 0, \end{aligned} \tag{10}$$

where the unknown spectral matrix $\mathbf{S}$ to be searched is linked to the partial measurements $\hat{\mathbf{S}}_{pp}^{m}$ by the sampling operator $\mathscr{A} : \mathbf{C}^{MP\times MP} \rightarrow \mathbf{C}^{MP\times MP}$ that extracts the elements from diagonal blocks, and the difference between $\mathscr{A}(\mathbf{S})$ and $\hat{\mathbf{S}}_{pp}^{m}$ in Frobenius norm is less than a given tolerance ε. $\mathbf{S}^* = \mathbf{S} \succeq 0$, in which $\succeq$ denotes positive semi-definite. The hermitian property is an inherent characteristic of spectral matrices, as well as the fact that its eigenvalues are non-negative. Unfortunately, it has no unique solution for block diagonal matrices of the type $\hat{\mathbf{S}}_{pp}^{m}$. An example is given here to illustrate this fact, and solid mathematical proof can be found in [3]. Assume that the measured matrix $\hat{\mathbf{S}}_{pp}^{m}$ is a 2-by-2 complex hermitian matrix $\begin{pmatrix} 1 & a^{-1} \\ a & 1 \end{pmatrix}$, where $a = \|a\|e^{j\varphi}$ is an unknown complex element and the diagonal elements are known measurements without error. By definition the objective matrix $\mathbf{S}$ is a rank-1 matrix and it is straightforward to find that $\|a\|e^{j\varphi} = \|a\|^{-1}e^{-j\varphi}$ as a result of hermitian symmetry. Therefore, the solution of Eq. (10) is non-unique since it can be written $\{a : \|a\| = 1, \forall\varphi\}$. Thus, another constraint is needed as explained in the next section.

3.2 Enforcing spatial continuity of the acoustic field

The spectral matrix reflects the correlation between the Fourier coefficients of the measurements, however, it does not contain information on the position of the microphones. For example, two adjacent columns in the spectral matrix must become equal if the corresponding microphones are infinitely close to each other (nearly overlapping) due to the spatial continuity of the acoustic field; accordingly, this information must be incorporated in the current problem. In this work, the spatial position of the microphones is encoded in the matrix completion problem by introducing an additional constraint. It is assumed that the measured pressure $\mathbf{p}$ with size $MP \times 1$ can be decomposed onto a dimension reduced spatial basis $\mathbf{\Phi} \in C^{MP\times K_p}$ ($K_p < MP$) with coefficients $\vartheta \in C^{K_p\times 1}$ as follows:

$$\mathbf{p} = \sum_{i=1}^{K_p} \phi_i(\mathbf{r})\vartheta_i = \mathbf{\Phi}\vartheta, \tag{11}$$

where $\phi_i(\mathbf{r})$ is the i-th column of matrix $\mathbf{\Phi}$ and ϑ_i is the i-th entry of vector ϑ. In this thesis, the Fourier basis is chosen, meaning that the acoustical field is decomposed as a sum of "acoustical modes" [14]. In other words, a spatial structure is encoded. The coefficients ϑ are related to the measurements as:

$$\vartheta = \mathbf{\Phi}^{\dagger}\mathbf{p}, \tag{12}$$

where † denotes the pseudoinverse of a matrix as a result $\mathbf{\Phi}$ is generally not invertible. Then the smoothed pressure $\tilde{\mathbf{p}}$ can be represented as [12]

$$\tilde{\mathbf{p}} = \mathbf{\Phi}\mathbf{\Phi}^{\dagger}\mathbf{p} = \mathbf{\Psi}\mathbf{p}, \tag{13}$$

where $\mathbf{\Psi} = \mathbf{\Phi}\mathbf{\Phi}^{\dagger}$ is defined as a projection operator. Now, let $\mathbf{S} \doteq \mathbb{E}\{\mathbf{p}\mathbf{p}^{*}\}$ and $\tilde{\mathbf{S}} \doteq \mathbb{E}\{\tilde{\mathbf{p}}\tilde{\mathbf{p}}^{*}\}$. Therefore,

$$\tilde{\mathbf{S}} = \mathbf{\Psi}\mathbf{S}\mathbf{\Psi}^{*}. \tag{14}$$

Equation (14) may be rewritten as $\|\mathbf{\Psi}\mathbf{S}\mathbf{\Psi}^{*} - \mathbf{S}\|_F \leq \varepsilon$ where ε is the representation error between $\mathbf{\Psi}\mathbf{S}\mathbf{\Psi}^{*}$ and $\mathbf{S}$ owing to the $\mathbf{\Phi}$ truncation. It is important that $\mathbf{\Psi}$ imposes a specific structure that encodes the information on microphone positions into the matrix $\mathbf{S}$. This can be seen as another constraint to be added to Eq. (10). It is noted that the $\mathbf{\Psi}$ is an orthogonal projection operator, which can be decomposed as $\boldsymbol{U}\begin{pmatrix} \mathbf{I}_{K_p} & 0 \\ 0 & 0 \end{pmatrix}\mathbf{U}^{*}$, where $\mathbf{U}\mathbf{U}^{*} = \mathbf{I}$, $\mathbf{I}_{K_p}$ is the identity matrix with n elements, and $\mathbf{U}$ is the modal matrix in the eigenvalue decomposition (EVD) of $\mathbf{\Phi}$. Then Eq. (13) can be written as

$$\tilde{\mathbf{p}} = \mathbf{\Psi}\mathbf{p} = \sum_{i=1}^{K_p} (\mathbf{p}^{*}\mathbf{u}_i)^{*}\mathbf{u}_i. \tag{15}$$

This means that only the $\mathbf{p}^{*}\mathbf{u}_i \;\; i = 1...K_p$ part corresponding to the eigenvalues equal to one are kept by this projection operator, and this is exactly the property of orthogonal projection operator. It is important to emphasize that the role of the orthogonal projection operator $\mathbf{\Psi}$ is to smooth the spectral matrix and to ensure the spatial continuity of the acoustical field.With the intension of defining the spatial basis $\mathbf{\Phi}$ in this projection basis, it is firstly denoted that K is the dimension of basis to represent the sound sources and MP is the total number of microphones by non-synchronous measurements. Then the Singular value decomposition (SVD) of the propagation function $\mathbf{H} \in \mathbb{C}^{MP\times K}$ between the array of non-synchronous measurements and sound sources is $\mathbf{H} = \mathbf{U}\mathbf{\Sigma}\mathbf{V}^{*}$ ($*$ denotes conjugate transpose), where $\mathbf{\Sigma}$, $\mathbf{U} \in \mathbb{C}^{MP\times MP}$, and $\mathbf{V} \in \mathbb{C}^{K\times K}$ are separately the singular values (a diagonal $MP \times K$ matrix with non-negative real numbers on the diagonal), left-singular vectors and right-singular vectors of $\mathbf{H}$. The physical meaning of the left-singular vectors are the "acoustical modes" to represent the acoustic field, and the right-singular vectors are the basis to represent the sources[6, 14]. Eventually, spatial basis $\mathbf{\Phi}$ is defined as $\mathbf{\Phi} = \mathrm{Ext}(\mathbf{U}, K_p)$, where the operator Ext extracts the first K_p columns of $\mathbf{U}$. K_p is chosen as $K_p = M\sqrt{P}$, which is a "rule of the thumb" as explained in Ref [1].

3.3 Low rank model of acoustic field with continuity constraint

The nuclear norm defined by a sum of the singular values of spectral matrix is an alternative relation of rank minimization. Thus, the data missing spectral matrix completion problem can

be then formulated as the following constrained optimization problem:

$$\begin{aligned} \underset{\mathbf{S}}{\text{minimize}} \quad & \|\mathbf{S}\|_* \\ \text{subject to} \quad & \|\mathscr{A}(\mathbf{S}) - \hat{\mathbf{S}}_{pp}^m\|_F \leq \varepsilon \\ & \|\mathbf{\Psi}\mathbf{S}\mathbf{\Psi}^* - \mathbf{S}\|_F \leq \varepsilon \\ & \mathbf{S}^* = \mathbf{S} \succeq 0, \end{aligned} \tag{16}$$

This optimization problem can be solved by the following FISTA algorithm [17]. The operator shrink is calculated as $\mathbf{U}\text{diag}(\max\{\sigma_i^2 - \lambda_k\mu, 0\})\mathbf{U}^*$, where $\max\{\sigma_i^2 - \lambda_k\mu, 0\}$ takes the maximum value between 0 and $\sigma_i^2 - \lambda_k\mu$, $\mathbf{U}$ and $\text{diag}(\sigma_i^2)$ are the elements of the Eigenvalue Decomposition (EVD) of matrix $\mathbf{G}_k$. A continuation technique is used here to tune the regularization parameter λ. It can be seen as a method to solve a sequence of problems (16) defined by an increasing sequence $\{\lambda_k\}$: (i) λ_0 as an initial regularization parameter and λ_d as final regularization parameter are chosen firstly; (ii) a high starting value of λ implies stronger regularization and the optimal manifold has a lower dimension and is easier to identify; (iii) a coarse to fine search is achieved in the solution space by decreasing the regularization parameter λ step by step (with a ratio η). The calculation procedure of FISTA is illustrated in Algorithm 1. The algorithm is stopped by the following criterion:

$$\frac{\|[\hat{\mathbf{S}}_{pp}^m]_{ij} - [\mathbf{G}_{k+1}]_{ij}\|_F}{\|[\hat{\mathbf{S}}_{pp}^m]_{ij}\|_F} \leq SC, \quad ij \in \mathbf{\Upsilon}, \tag{17}$$

where SC is a constant value that is chosen by the user, $[]_{ij}$ denotes the (i, j) element of a matrix and $\mathbf{\Upsilon}$ the positions of fixed block diagonal entries.

Algorithm 1 Nuclear Norm minimization by FISTA

1: Starts with $\mathbf{G}_0 = \mathbf{S}_0 = 0 \in \mathbb{C}^{MP\times MP}$, $t_1 = 1$; μ is step size, λ_0 is an initial regularization parameter and λ_d is the final regularization parameter, and η is the radio to decrease λ_{k-1} in each step.
2: **While** $\lambda_k \geq \lambda_d$ **do**
3: **For** $1 : N_m$ (N_m is the maximum iteration steps for each regularization)
4: $\mathbf{G}_k = \mathbf{G}_{k-1} - \mu(\mathscr{A}(\mathbf{G}_{k-1}) - \hat{\mathbf{S}}_{pp}^m)$
5: $\tilde{\mathbf{S}}_k = \text{shrink}(\mathbf{G}_k, \lambda_k\mu)$
6: $\boldsymbol{S}_k = \mathbf{\Psi}\tilde{\boldsymbol{S}}_k\mathbf{\Psi}^*$
7: $t_{k+1} = \frac{1}{2}(1 + \sqrt{1 + 4t_k^2})$
8: $\mathbf{G}_{k+1} = \mathbf{S}_k + \frac{t_k - 1}{t_{k+1}}(\mathbf{S}_k - \mathbf{S}_{k-1})$
9: **End**
10: **If** Stopping criteria $\leq SC$,
11: **break**
12: **End for if**
13: $\lambda_k = \max(\eta\lambda_{k-1}, \lambda_d)$
14: Go to step 2.

4 SIMULATION ANALYSIS

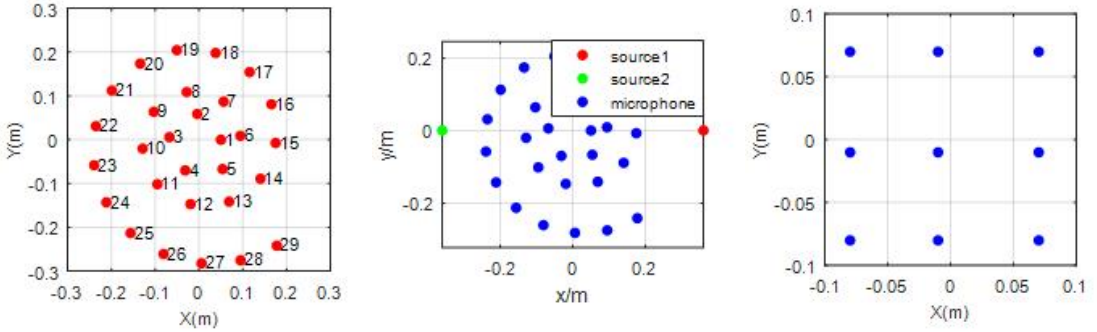

(a) (b) (c)

Figure 2: The positions of microphone array: (a) a 29-element Dougherty spiral array, (b) the relative position of sources and spiral array, (c) the center positions of 9 times non-synchronous measurements.

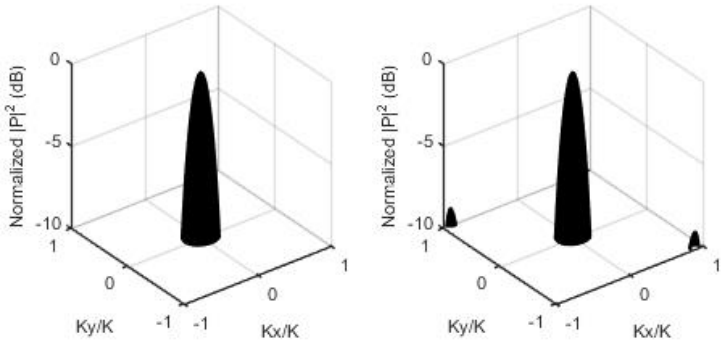

(a) (b)

Figure 3: Far-Field array pattern: (a) 2.8kHz, (b) 2.9kHz.

In order to design a far field array, the array resolution and spatial aliasing must be taken into account. Array resolution specifies how well an array is able to resolve the direction of propagation. It is typically specified in terms of a 3 dB down point from the peak at which the spatial filter formed by an array processing algorithm. The width of the spatial filter at the 3 dB down point is the beamwidth, which determines the array resolution of conventional beamforming. Spatial aliasing is an undesirable side effect from spatially under-sampling the aperture of an array. The primary challenge with array designs is that they must work well for a broad range of frequencies. The lowest frequencies of interest drive the array aperture

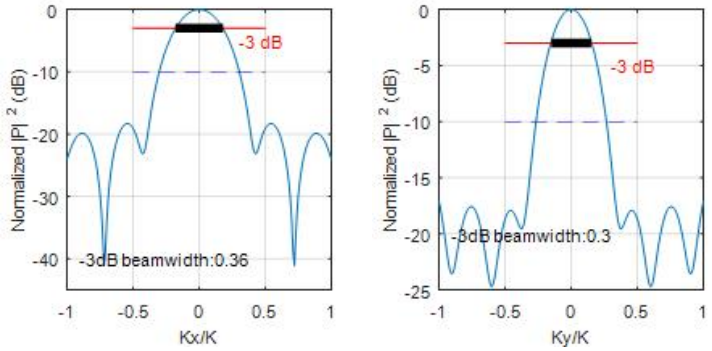

(a) (b)

Figure 4: Far-Field array pattern at 2kHz: (a) profile representation along the kx(x) direction, (b) profile representation along the ky(y) direction.

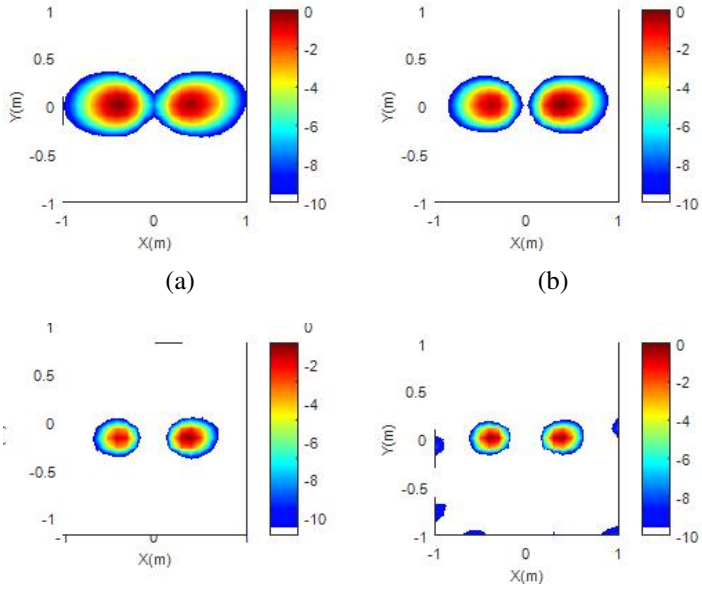

(a) (b)

(c) (d)

Figure 5: Sound source imaging result at different frequencies of single measurement of (a) 1.8kHz, (b) 2kHz, (c) 2.8kHz, (d) 3kHz.

size larger to obtain adequate source resolution. The highest frequencies drive the intra-sensor spacing smaller due to the classical half-wavelength requirement for eliminating spatial aliasing.

In this paper, a spiral array is designed by equally spacing the array sensors on a logarithmic spiral, which provides a broad base of inter-sensor spacings, and a 29-element Dougherty spiral array of used in this paper is shown in Fig. 2 (a). The sidelobe characteristics of the Dougherty

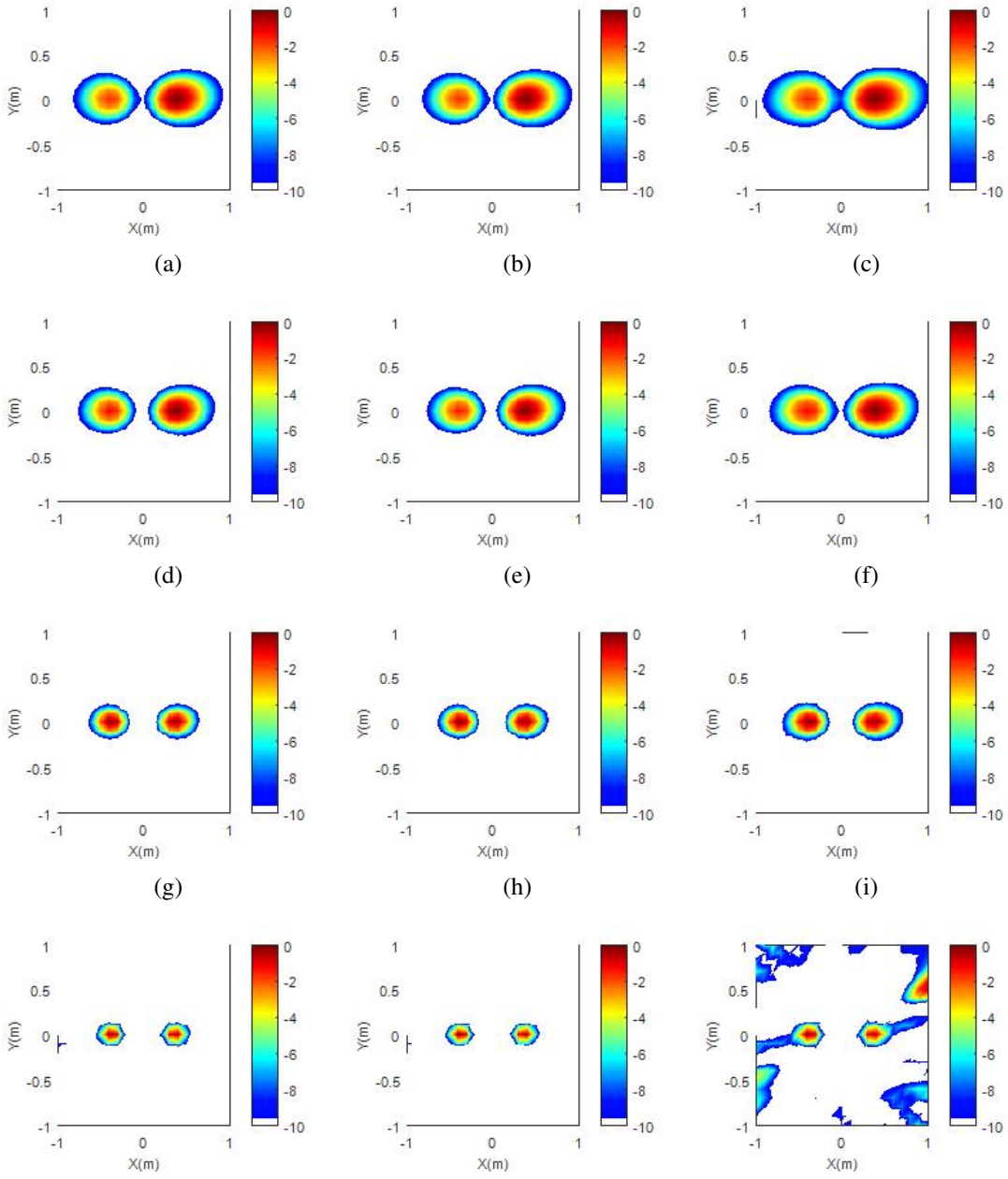

Figure 6: Sound source imaging result of (a) non-synchronous measurements of 9 times at 1.6kHz, (b) simultaneous measurements at 1.6kHz, (c) single measurements at 1.6kHz, (d) non-synchronous measurements of 9 times at 2kHz,(e) simultaneous measurements at 2kHz, (f) single measurements at 2kHz, (g) non-synchronous measurements of 9 times at 2.8kHz, (h) simultaneous measurements at 2.8kHz, (i) single measurements at 2.8kHz, (j) non-synchronous measurements of 9 times at 4.5kHz,(k) simultaneous measurements at 4.5kHz,(l) single measurements at 4.5kHz.

spiral array at an extreme range of frequency are shown in Fig. 3. Figure 3 (a) shows the sidelobe is 10 dB smaller than the peak at 2.8 kHz, therefore it can be ignored. Figure 3 (b) shows that the sidelobe appeared in dynamic range of 10 dB at 2.9 kHz, which causes the spatial aliasing in the imaging results of beamforming. To avoid spatial aliasing, the highest working frequency of current array is 2.8kHz. With the purpose of determine the working frequency of lowest, the beamwidth of the Dougherty spiral array is shown in Fig. 3. The relative positions between the sources and array is shown in Fig. 2(b), and with the sources at a spacing of 0.76m, the lowest frequency of working of the current array is 2kHz. This is verified by the beamwidth of 0.36 along kx(x) and 0.3 along ky(y) at 2kHz, which are shown in Fig. 4. The center positions of the non-synchronous measurements are shown in Fig. 2 (c), 9 times non-synchronous measurements are applied in the current setup. Figure 6 shows the results of acoustic imaging in non-synchronous measurements, simultaneous and single measurements respectively. It is observed that the non-synchronous measurements broaden the frequency range of working from $2-2.8$ kHz to $1.6-4.5$ kHz. The imaging results of single measurement (with only an array of 29 elements) are non-distinguishable when it is applied outside the frequency range of $2-2.8$ kHz. However, the imaging results of non-synchronous measurements (with only an array of 29 elements and moving 9 times sequentially) keep distinguishable in the range of $1.6-4.5$ kHz, which are comparable with the simultaneous measurements of array of 261 elements.

5 CONCLUSION

In this paper, non-synchronous measurements beamforming is formulated as a spectral matrix completion problem which is solved by minimizing the nuclear norm of a spectral matrix subject to measurements fitting, Hermitian symmetry, and spatial continuity of the sound field. The proposed non-synchronous measurements beamforming extended greatly the working frequency range of a single array measurement. The simulation results show the non-synchronous measurements beamforming extended the working frequency range of given small phased array from $2-2.8$ kHz to $1.6-4.5$ kHz with only 9 times non-synchronous measurements. It is verified that the non-synchronous measurements improve the frequency range of working with limited number of microphones, which improve the capability of array and reduce the budget of measurements greatly in the aspects of number of microphones and channels of acquisition system.

6 ACKNOWLEDGEMENTS

The authors would like to thank the continuous discussion with Ms.Wenhuang Wang and Jianzheng Gao (Shanghai Jiao Tong University). This work was supported by the National Natural Science Foundation of China (Grant No. 11704248).

References

[1] J. Antoni, Y. Liang, and Q. Leclère. “Reconstruction of sound quadratic properties from non-synchronous measurements with insufficient or without references: Proof of concept.”

Journal of Sound and Vibration, 349, 123–149, 2015.

[2] C.-X. Bi, W.-Q. Jing, and Y.-B. Zhang. "Broadband acoustic holography from intensity measurements with a three-dimensional pressure-velocity probe." *The Journal of the Acoustical Society of America*, 138(5), 2929–2936, 2015.

[3] E. Candès and B. Recht. "Exact matrix completion via convex optimization." *Foundations of Computational Mathematics*, 9(6), 717–772, 2009.

[4] R. P. Dougherty. "What is Beamforming?" In *Proceedings on CD of the 2nd Berlin Beamforming Conference, 19-20 February, 2008*. GFaI, Gesellschaft zu Frderung angewandter Informatik e.V., Berlin, 2008. ISBN 978-3-00-023849-9. URL `http://bebec.eu/Downloads/BeBeC2008/Papers/BeBeC-2008-01_Dougherty.pdf`.

[5] Y. Kim and P. Nelson. "Optimal regularisation for acoustic source reconstruction by inverse methods." *Journal of Sound and Vibration*, 275(35), 463 – 487, 2004. ISSN 0022-460X.

[6] Q. Leclère. "Acoustic imaging using under-determined inverse approaches: Frequency limitations and optimal regularization." *Journal of Sound and Vibration*, 321(35), 605 – 619, 2009. ISSN 0022-460X.

[7] Y. Liang. *Acoustical source reconstruction from non-synchronous sequential measurements*. Ph.D. thesis, INSA de Lyon, 2015.

[8] T. Loyau, J.-C. Pascal, and P. Gaillard. "Broadband acoustic holography reconstruction from acoustic intensity measurements. i: Principle of the method." *The Journal of the Acoustical Society of America*, 84(5), 1744–1750, 1988.

[9] W. Lu, W. Jiang, G. Yuan, and L. Yan. "A gearbox fault diagnosis scheme based on near-field acoustic holography and spatial distribution features of sound field." *Journal of Sound and Vibration*, 332(10), 2593 – 2610, 2013. ISSN 0022-460X.

[10] U. Michel. "History of acoustic beamforming." In *Proceedings on CD of the 1st Berlin Beamforming Conference, 22-23 November, 2006*. GFaI, Gesellschaft zu Frderung angewandter Informatik e.V., Berlin, 2006. ISBN 978-3-00-019998-1. URL `http://www.bebec.eu/Downloads/BeBeC2006/Papers/BeBeC-2006-01_Michel.pdf`.

[11] A. Nejade. "Reference-less acoustic holography techniques based on sound intensity." *Journal of Sound and Vibration*, 333(16), 3598–3608, 2014.

[12] J.-C. Pascal, S. Paillasseur, J.-H. Thomas, and J.-F. Li. "Patch near-field acoustic holography: Regularized extension and statistically optimized methods." *The Journal of the Acoustical Society of America*, 126(3), 1264–1268, 2009.

[13] C. Pézerat, Q. Leclère, N. Totaro, and M. Pachebat. "Identification of vibration excitations from acoustic measurements using near field acoustic holography and the force analysis technique." *Journal of Sound and Vibration*, 326(35), 540 – 556, 2009. ISSN 0022-460X.

[14] D. M. Photiadis. "The relationship of singular value decomposition to wave-vector filtering in sound radiation problems." *The Journal of the Acoustical Society of America*, 88(2), 1152–1159, 1990.

[15] E. G. Williams. *Fourier acoustics: sound radiation and nearfield acoustical holography*. Academic press, 1999.

[16] L. Yu, J. Antoni, and Q. Leclère. "Spectral matrix completion by cyclic projection and application to sound source reconstruction from non-synchronous measurements." *Journal of Sound and Vibration*, 372, 31 – 49, 2016. ISSN 0022-460X.

[17] L. Yu, J. Antoni, Q. Leclere, and W. Jiang. "Acoustical source reconstruction from non-synchronous sequential measurements by fast iterative shrinkage thresholding algorithm." *Journal of Sound and Vibration*, 408, 351–367, 2017.